Nanoscopic fluctuational dynamic model of anomalous temperature and concentration dependences in the Sn Mössbauer isomer shift in Ag-Sn alloys

2000 J. Phys.: Condens. Matter 12 7275

(http://iopscience.iop.org/0953-8984/12/32/311)

J. Phys.: Condens. Matter **12** (2000) 7275–7285. Printed in the UK PII: S0953-8984(00)14610-7

Nanoscopic fluctuational dynamic model of anomalous temperature and concentration dependences in the Sn Mössbauer isomer shift in Ag–Sn alloys

Yu L Khait†, I B Snapiro†, H Shechter† and D Haskel‡

† Solid State Institute, Technion–Israel Institute of Technology, Haifa 32 000, Israel
‡ Physics Department, Box 351560, University of Washington, Seattle, WA 98195, USA

Received 9 June 2000

Abstract. A nanoscopic fluctuational dynamic model is suggested for observed anomalous reversible changes of the Mössbauer isomer shift (ARCOMIS) found recently in Ag–Sn alloys not affected by long ageing. The model considers fluctuation-induced nanoscale large transient atomic displacements (LTADs) and material disordering. They cause electron localization, taking place simultaneously and permanently in the nanometre vicinities of Mössbauer impurity atoms in the entire alloy. This causes an additional enhancement in the electron charge density $|\Psi_f(0)|^2$ at the Mössbauer nuclei, leading to the ARCOMIS at temperature T_s. These phenomena are generated by persistent sequences of nanoscale short-lived (picosecond) large energy fluctuations (SLEFs) of atomic particles of the peak thermal energy $\epsilon_{0p} > \Delta E \gg kT$, which occur simultaneously and constantly in the material. The model leads to the following results. (i) A SLEF-mediated dynamic mechanism for the ARCOMIS occurring at relatively low temperatures T_s is proposed. (ii) The temperature T_s(Ag–Sn) $\approx$ 500 K is calculated, in good agreement with observations. (iii) The narrow temperature interval $\delta T \ll T_s$ within which the ARCOMIS takes place (around T_s) is calculated, in good agreement with observations. (iv) The magnitude of the ARCOMIS is calculated, in agreement with observations. (v) An explanation of why the ARCOMIS is observed only at Sn concentrations b(Sn) $> 3\%$ is suggested. (vi) An explanation is offered for the absence of the ARCOMIS in SnO_2 material. (vii) Similar results are obtained for the Au–Sn alloys not affected by long ageing, in good agreement with tentative experimental data.

1. Introduction

The questions of the local thermal dynamics of impurity atoms and local material stability around them in binary alloys have been addressed recently by many workers [1–9]. One of the most interesting reported results of these studies was the discovery of dynamic anomalies in the thermal motion of individual impurity atoms in binary alloys. Earlier the anomalies in the thermal motion of the Mössbauer impurity atoms were found to manifest themselves in the observed anomalies in the Mössbauer spectral intensity in Ag–Sn, Au–Sn and Pb–Sn alloys [4, 5] at temperature T_0 substantially lower than the melting point T_m. Recently new temperature and Sn concentration anomalous dependences in the Mössbauer isomer shift (IS) in Ag–Sn alloys have been observed around a certain temperature $T_s < T_0$ within a narrow temperature interval $\delta T_s \ll T_s$ [8]. The observed dynamic anomalies in the motion of the Mössbauer impurity atoms and the related observed anomalies in the Mössbauer spectroscopy could not be explained in terms of the standard theory of the Mössbauer effect [10, 11] which considers ordinary quasiharmonic (and weakly anharmonic) thermal atomic oscillations of small displacements $\sigma_A \ll d$ (d is the average interatomic spacing). This situation has

0953-8984/00/327275+11$30.00

motivated us to apply to the aforementioned problems a qualitatively new approach which first was used to suggest an explanation for the observed anomalies in the Mössbauer spectral intensity [9]. The approach is based on the nanoscopic kinetic electron-related many-body theory of short-lived large energy fluctuations (SLEFs) of single atoms (or a small number $N_0 > 1$ of atoms) in solids applied successfully to a broad range of processes in various materials [12–30]. The SLEF theory takes into account SLEF-generated highly anharmonic large transient atomic displacements $\Delta q \gg \sigma_A$, and related strong electron–lattice interactions able to generate significant non-adiabatic electron rearrangements which are considerably different from the conventional electron–phonon interactions. Just these SLEF-generated strong electron–lattice interactions which cause many large observed (sometimes anomalous) effects [9, 12, 13, 15, 17–23, 25–29], suggest an explanation for recently found [8] anomalies in the Mössbauer isomer shift, as we discuss in detail in the following sections.

In this paper we extend the SLEF-based model proposed in [9] in order to suggest a dynamic mechanism for the observed anomalous reversible changes of Mössbauer isomer shift (ARCOMIS) and its dependences on temperature and Sn concentration in Ag–Sn alloys unaffected by long ageing described in [8].

The proposed model also enables one to calculate the temperature T_s around which the ARCOMIS occurs and a narrow temperature interval $\delta T \ll T_s$ within which the ARCOMIS takes place, as well as the magnitude of the anomalous line shift, in agreement with experimental data.

2. Statement of the problem

We start from the consideration of some essential differences between the observed ARCOMIS found in Ag–Sn alloys unaffected by long ageing [8], on the one hand, and the conventional isomer shift, on the other. The latter, determined by the difference of the local static electron configurations in the vicinity of the Mössbauer impurity atoms in the source and absorber, is

$$\Delta U_{IS} = \alpha(|\Psi_a(0)|^2 - |\Psi_s(0)|^2). \tag{2.1}$$

Here $|\Psi_a(0)|^2$ and $|\Psi_s(0)|^2$ are the electron charge densities (ECDs) at the absorber and source nuclei, respectively. The parameter α is a constant and contains a factor $\delta R/R$ which reflects the relative difference δR of the nuclear radius R between the excited and ground state of the Mössbauer nucleus. Thus the constant α depends on the nuclear parameters *only* and is independent of the environment of the Mössbauer impurity atoms.

The factor in the parenthesis in equation (2.1) depends on the electron configuration and parameters in the environment of the active nuclei. The conventional theory of the Mössbauer SI takes into account only the *static* change in the local electron configuration in the vicinity of the Mössbauer atoms and in the ECD $|\Psi_a(0)|^2$ at the Mössbauer nuclei caused by an alternating of chemical composition in the neighbourhood of these nuclei. However, experimental studies of Ag–Sn alloys [8] have shown some additional anomalous reversible change of the Mössbauer isomer shift which occurs within a narrow temperature interval $\delta T \ll T_s$ around a relatively low temperature $T_s \approx 500$ K. The ARCOMIS was found in binary metallic alloys of Ag–Sn that had not been aged for a long time. In this case the observed changes in the IS appeared to be reproducible while affected by heating–cooling cycles. It is important to note that the ARCOMIS-related rather sharp changes in the line shift within a narrow temperature interval $\delta T \ll T_s$ (recalling phase-transition-like changes) take place at a relatively low temperature T_s (even lower than the temperature T_0 (Ag–Sn) at which the anomalies in the Mössbauer spectral intensity were observed [4, 5, 9]), around which no known phase or structural transformations occur in Ag–Sn alloys. Moreover, the ARCOMIS was observed in Ag–Sn alloys at 4 and

8% of Sn impurities and was not detected at 1 and 2% of Sn atoms in these metal alloys. It should be emphasized that both 4 and 8% concentrations of Sn in the Ag–Sn alloys at which the ARCOMIS is observed are lower than the solubility limit of Sn in Ag. This means that the phase (or structural) transformations (such as the Sn crystallization) do not occur. It is worthwhile mentioning that at the Sn concentrations $b(\mathrm{Sn}) > 3\%$, at which the ARCOMIS is observed, a noticeable fraction of Ag atoms have Sn atoms as their nearest neighbours, whereas at lower Sn concentrations $b_L(\mathrm{Sn}) < 3\%$, at which the ARCOMIS has not been detected, the above conditions are broken. In the experimental conditions leading to the ARCOMIS there is also no reason to expect the formation of Sn clusters of macroscopic sizes that can cause the observed anomalies. The origin of the observed ARCOMIS as well as its dependence on temperature and Sn concentration differing considerably from the conventional IS are not understood through traditional wisdom. According to the way we understand the IS, the observed ARCOMIS and its dependences on temperature and Sn concentration indicate that some unconventional phenomena cause an additional enhancement in the electron charge density on the Sn nuclei around temperature T_s.

In this paper we suggest that the ARCOMIS is generated by persistent sequences of a great number of nanoscale short-lived large energy fluctuations (SLEFs) of atomic particles, SLEF-generated large transient atomic displacements (LTADs) and strong electron–lattice interactions taking place simultaneously and permanently in the solids. These phenomena are similar to those which cause the anomalies in the Mössbauer spectral intensity [9] and some other phenomena in solids [12, 17, 23, 24]†. In the following sections we consider these persistent random sequences of a great number of correlated nanometre SLEFs and SLEF-generated highly non-linear LTADs $\Delta q \geqslant \delta \gg \sigma_A$ and related strong electron–lattice interactions. They cause electron localizations in nanometre vicinities of Sn atoms, which occur simultaneously and permanently in the material. These phenomena are able to change 'anomalously' the ECD $|\Psi_f(0)|^2$ at the Mössbauer nuclei and thus to generate the observed ARCOMIS.

It should be emphasized that the proposed model is not an *ad hoc* model designed specially for the consideration of anomalous phenomena found in Mössbauer spectroscopy. The SLEF-based models using the highly anharmonic LTADs and strong electron–lattice interactions, which cause strongly correlated atomic and electronic motions, have been successfully used earlier for the consideration of many phenomena (including so-called 'anomalous' ones) in various materials and systems [9, 12–30].

3. Dynamic nanoscopic model for large correlated fluctuations in atomic displacements and electron density at the Mössbauer nuclei

Since the theory of short-lived (picosecond) energy fluctuations (SLEFs) in nanometre regions of solids and its applications are well documented in the literature [9, 12–30], we summarize here only some key points of the SLEF theory related to SLEFs and SLEF-induced atomic and electronic phenomena causing anomalies in the Mössbauer isomer shift. We start by summarizing the main assumptions adopted in the conventional theory of solids [31–34] and

† The transient correlated motion of the $N_0 \geqslant 1$ strongly fluctuating particles of thermal energy $\epsilon_{0p} \gg N_0 kT$ and of many surrounding particles located in the nanometre vicinity (during a SLEF) is described in terms of time-dependent local distribution functions of the involved particles and local kinetic parameters. These functions are governed by coupled kinetic integrodifferential equations obtained from the time-dependent Liouville equation (in [12, 17]). In the present work we do not consider the SLEF kinetic equations. Instead, we use their solution and semiphenomenological estimates of parameters describing large SLEF-induced displacements of atoms and the correlated atomic and electronic motion in nanometre material regions affected by SLEFs which cause the observed anomalies in the Mössbauer line shift.

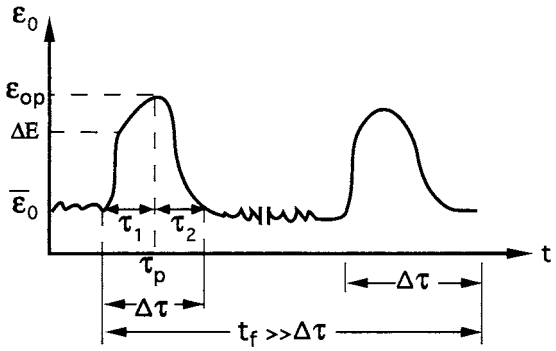

Figure 1. Time and energy scales of two successive reversible short-lived large energy fluctuations (SLEFs) of $N_0 \geqslant 1$ atoms up to the peak thermal energy $\epsilon_{0p} \geqslant \Delta E(\delta) \gg kT$, $\Delta\tau = 10^{-13}$–10^{-12} s is the SLEF lifetime, $\tau_1 \approx \Delta\tau/2$ is the SLEF formation time, $\tau_2 \approx \tau_1$ is the SLEF relaxation time; τ_p is the instant of the SLEF peak; t_f is the average time between two successive SLEFs of the same atoms.

used in the traditional theory of the Mössbauer effect [10, 11]. These assumptions broken by SLEFs and SLEF-generated highly non-linear non-equilibrium phenomena are the following.

(i) *Average atomic displacements σ_A are small* compared to the average interatomic spacing d.
(ii) *The electron motion can be separated (in the first approximation) from the atomic motion* through the Born–Oppenheimer adiabatic approximation due to the above assumption $\sigma_A \ll d$.
(iii) The collective atomic motion may be described in terms of the *harmonic (quasiharmonic) approximation and phonons due to the condition $\sigma_A \ll d$.*
(iv) The electron–lattice interactions are usually described in terms of electron–phonon interactions assuming $\sigma_A \ll d$.

The aforelisted assumptions, although proved extremely effective in numerous fields, impose strong limitations on the consideration of a broad range of phenomena associated with SLEF-generated large transient atomic displacements (LTADs) $\Delta q_0 = |q_0 - \bar{q}_0| \gg \sigma_A$ (from the mean atomic positions $\bar{q}_0$), the related highly anharmonic atomic motion and strong electron–lattice interactions. The limitations of the conventional solid state theory imposed by the assumption of the smallness of atomic displacements were first stressed by Frenkel [35] about 50 years ago. The theory of SLEFs and SLEF-related phenomena frees one from the above assumptions [9, 12–29, 36]. This enables one to take into account the effects of SLEF-generated LTADs $\delta \gg \sigma_A$ and strong electron–lattice interactions, leading to interrelated atomic and electronic dynamic distortions in the vicinities of impurity atoms which cause the Mössbauer line shift.

The time and energy scales of single SLEFs are shown in figure 1. Individual reversible SLEFs of the peak thermal energy $\epsilon_{0p} \geqslant \Delta E \gg kT$ have the lifetime $\Delta\tau = \tau_1 + \tau_2 = 10^{-13}$–$10^{-12}$ s. $\Delta\tau$ includes the SLEF formation time $\tau_1 \approx 0.5\Delta\tau$ and SLEF relaxation time $\tau_2 \approx \tau_1$. During τ_1 (preceding the instant τ_p of the SLEF peak), the $N_0 \approx 1$ SLEF-generated hyperthermal fluctuating atoms (HFAs) receive the thermal energy $\epsilon_{0p} \gg kT$ only from the HFA's nanometre vicinity of radius $R_1 \approx c_s\tau_1 \approx 10^{-7}$ cm and volume $\Omega_1 \approx 4R_1^3 \gg d^3$ (c_s is of the order of the sound velocity). The volume Ω_1 contains $\Delta N_1 \gg N_0 \approx 1$ atoms, typically $\Delta N_1 \approx$ 20–100 for different ϵ_{0p} and material parameters [9, 12–19]. During τ_1 the ΔN_1 atoms surrounding the HFAs are 'cooled' down by 10–20%. Thus during τ_1 the total number $N_1 = N_0 + \Delta N_1 \approx \Delta N_1$ of atoms located in the nanometre volume $V_1 = V_0 + \Omega_1 \approx 4R_1^3$

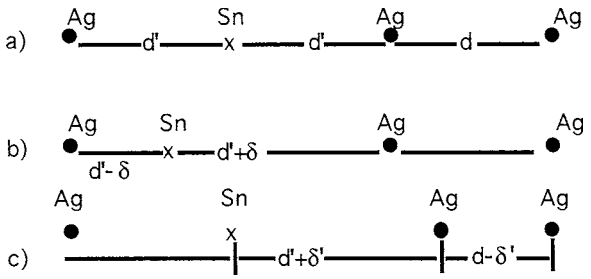

Figure 2. A one-dimensional diagram of the SLEF-induced large transient atomic displacements (LTADs) $\delta \gg \sigma_A$. (a) Equilibrium local atomic configuration in the Ag–Sn alloy in the absence of SLEFs. (b) SLEF-generated LTAD $\delta \gg \sigma_A$ of an Sn atom of picosecond duration. (c) SLEF-generated LTAD of an Ag atom neighbouring the Mössbauer Sn atom. The LTAD stretches one interatomic distance and simultaneously shrinks another one.

are involved in the creation of the local non-equilibrium nanometre region containing HFAs, LTADs and large correlated atomic and electronic distortions. $V_0 \approx N_0 d^3 \ll \Omega_1$ is the volume occupied by the $N_0 \approx 1$ fluctuating atoms. The SLEF-generated distortions in the nanometre region form a transient point dynamic defect of lifetime $\Delta\tau = \tau_1 + \tau_2$. During the SLEF relaxation time $\tau_2 \approx \tau_1$ the HFAs give the 'borrowed' energy back to the ΔN_1 surrounding atoms in $\Omega_f^1 \approx \Omega_f$, and thus the HFAs, LTADs and large local lattice distortions disappear. The LTADs $\Delta q \geqslant \delta \gg \sigma_A$ of Sn and Ag atoms generated by a single SLEF are shown schematically in figure 2, and they can also be seen in molecular dynamic simulations [16, 17]. The SLEF-induced large local interrelated transient atomic and electronic distortions in the nanometre regions generate strong electron–lattice interactions differing considerably from the conventional electron–phonon interactions. The SLEF-generated electron–lattice interactions can cause non-adiabatic electron transitions, transient electron localizations in the nanometre vicinity of Mössbauer atoms (and other related phenomena manifesting themselves in a broad range of phenomena in various materials [9, 12–15, 17–30, 36]). The probability (per second and per atom) of SLEFs of $\epsilon_{0p} \geqslant \Delta E \gg kT$ (and thus of the SLEF generated LTADs and electron localizations) obtained from the kinetic consideration [12, 16, 17]

$$W = \Delta\tau^{-1} \exp(-\Delta G/kT) \tag{3.1}$$

is similar to that used in our previous work [9]. Here $\Delta G = \Delta E - T(\Delta S_{0p} + \delta S)$ is the effective SLEF activation free energy, ΔS_{0p} is the entropy caused by SLEF-induced local atomic disordering in the nanometre region, $\delta S \approx k(\Delta n^{up} - \Delta n^d)$ is the entropy change caused by Δn^{up} upward and/or Δn^d downward electron transitions generated by the SLEF and related SELI. $\epsilon_{0p} \geqslant \Delta E \gg kT$ and $\Delta E(\delta)$ is the SLEF threshold energy sufficient to produce the LTADs $\Delta q_0 \geqslant \delta \gg \sigma_A$ but insufficient to generate atomic jumps over energy barriers (figure 2). The SLEF-generated LTADs and transient point dynamic defects cause electron localization in the Mössbauer atom nanometre vicinity [9, 12, 17]. This enhances the ECD $|\Psi_f(0)|^2$ at the Mössbauer nuclei compared to the ECD $|\Psi_a(0)|^2$ in the absence of the LTADs in the absorber as shown in figure 3. As a result, every individual SLEF generates the additional Mössbauer line shift

$$\Delta U_f = \alpha(|\Psi_f(0)|^2 - |\Psi_a(0)|^2) > 0 \tag{3.2}$$

at the Mössbauer nuclei located in the SLEF-affected nanometre regions.

Up to now we considered properties of individual SLEFs and related phenomena. Now we shall take into account the permanent existence in the material of persistent random sequences of 'successive generations' of a great number of simultaneously occurring SLEFs (and the

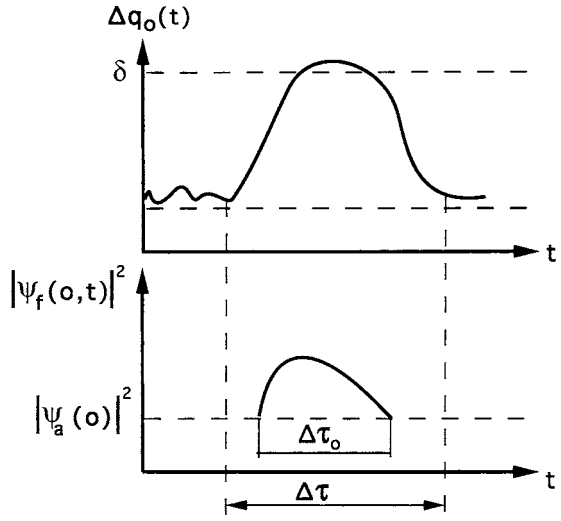

Figure 3. A diagram of a SLEF-induced large transient atomic displacement (LTAD) $\Delta q_0 \geqslant \delta \gg \sigma_A$ in the vicinity of the Mössbauer atom and the corresponding transient enhancement $|\Psi_f(0)|^2 - |\Psi_a(0)|^2$ in the electron charge density (ECD) $|\Psi_f(0)|^2$ at the Mössbauer nucleus of picosecond duration $\Delta\tau_0 \leqslant \Delta\tau$; here $|\Psi_a(0)|^2$ and $|\Psi_f(0)|^2$ are the ECD in the absence and presence of the SLEF.

SLEF-generated hyperthermal atoms, LTADs $\Delta q_0 \gg \sigma_A$ and related electron localization in the vicinity of Mössbauer atoms) which exist constantly in the material. The average number per cm^3 of simultaneously and constantly occurring SLEFs and SLEF-generated phenomena is [9, 12, 17, 23–25]

$$\eta_f(\Delta E, T) = d^{-3}\exp(-\Delta G/kT). \tag{3.3}$$

Each of the SLEFs creating the LTADs (figure 2) and related localized electrons around the Mössbauer atom is able to initiate an ECD enhancement ($|\Psi_f(0)|^2 - |\Psi_a(0)|^2$) at the Mössbauer nuclei (figure 3). Therefore, the studied alloys should contain the Sn concentration $b(\mathrm{Sn}) \geqslant 3\%$ in order to ensure the presence of the Mössbauer Sn atoms in all SLEF-excited nanometre regions each of which contains $N_1 \approx$ 30–100 atoms [9, 12–19]. In this case the average distance between Sn atoms

$$\Delta r(\mathrm{Sn}) \leqslant d[b(\mathrm{Sn})]^{-1/3} \approx 3d \tag{3.4}$$

is of the order of the size $N_1^{1/3}d$ of the individual SLEF-affected nanometre regions, and the conditions

$$b(\mathrm{Sn})N_1 \geqslant 1 \qquad N_1^{1/3}d \approx \Delta r(\mathrm{Sn}) \text{ or } [b(\mathrm{Sn})N_1]^{1/3} \approx 1 \tag{3.5}$$

are satisfied. Under these conditions the nanometre regions excited simultaneously and permanently by SLEFs of $\epsilon_{0p} \geqslant \Delta E$ contain the Mössbauer nuclei. They are affected by the SLEF-generated ECD enhancements ($|\Psi_f(0)|^2 - |\Psi_a(0)|^2$) (figure 3) manifesting themselves in the ARCOMIS. The average cubic density of Sn-containing SLEF-excited nanometre regions in which the SLEF-generated ECD enhancements ($|\Psi_f(0)|^2 - |\Psi_a(0)|^2$) take place simultaneously and permanently is

$$\eta_s(\Delta E, T, b) = \eta_f(\Delta E, T)b(\mathrm{Sn})N_1 = d^{-3}b(\mathrm{Sn})N_1\exp(-\Delta G/kT). \tag{3.6}$$

The average distance between such regions is

$$r_s(\Delta E, T, b) \approx [\eta_s(\Delta E, T, b)]^{-1/3} \approx [b(\mathrm{Sn})N_1]^{-1/3}r_f(\Delta E, T). \tag{3.7}$$

At low T the cubic density $\eta_s(\Delta E, T, b)$ is small, and the distance $r_s(\Delta E, T, b)$ between the SLEF-affected Sn nuclei is much larger than the diameter $2R_1 \approx 10^{-7}$ cm of the SLEF-related nanometre material region $V_1 \approx 4R_1^3$. Therefore, at such low T when the relatively small density η_s of Sn nuclei is concurrently affected by the SLEF-induced LTADs $\Delta q_0 \geqslant \delta$ (figure 2) and ECD enhancements (figure 3) the detectable line shift is not produced. However, when temperature T in the absorber rises, the distance $r_s(\Delta E, T, b)$ between the nanometre regions containing the Mössbauer nuclei affected simultaneously and permanently by SLEF-generated ECD enhancements $(|\Psi_f(0)|^2 - |\Psi_a(0)|^2)$ decreases exponentially (equations (3.6) and (3.7)). As a result, these co-existing SLEF-affected nanometre regions (and Mössbauer Sn nuclei within them) start to correlate with one another and form clusters. Then within a narrow temperature interval $\delta T \ll T_s$ around a certain temperature T_s this dynamic percolation-like process reaches its critical stage. In this case the distance $r_s(\Delta E, T, b)$ reaches its critical nanometre value (of the order of the diameter $2R_1 \approx 10^{-7}$ cm), satisfying the critical condition

$$r_s(\Delta E, T_s, b) = 2\alpha R_1 = Ad \qquad \text{with } A = 2\alpha R_1/d \gg 1. \tag{3.8}$$

Here $\alpha \geqslant 1$ is referred to as the percolation parameter. This SLEF-induced dynamic percolation process, producing the detectable ARCOMIS within a narrow temperature interval $\delta T \ll T_s$, is similar to those causing the phase-transition-like anomalies in the Mössbauer spectral intensity [9] and other phase and structural transformations [12, 17, 23, 24].

From equations (3.6), (3.7) and (3.8) we find the critical temperature T_s around which the ARCOMIS takes place

$$T_s = \frac{\Delta E}{k}\left[\frac{\delta S + \Delta S_{0p}}{k} + 3\ln[A(b(\mathrm{Sn})N_1)^{1/3}]\right]^{-1}. \tag{3.9}$$

Here we used the relation for the SLEF-related free energy $\Delta G = \Delta E - T(\Delta S_{0p} + \delta S)$ discussed above in connection with equation (3.1) and the condition $T = T_s$. The SLEF threshold energy ΔE can be calculated from the following relation:

$$\Delta E(\delta) = (\delta/d)^2 B\Omega_0 \tag{3.10}$$

similar to that used in [9, 12, 15, 17, 23]. Here B is the bulk modulus and Ω_0 is the average volume per atom. One can expect that SLEF-induced LTADs $\Delta q_0 \geqslant \delta$ (figure 2) producing the ARCOMIS are slightly lower than the SLEF-generated LTADs $\Delta q_0' \geqslant \delta_0 \approx 0.2d$ which cause temperature anomalies in the Mössbauer spectral intensity [9], and that the condition

$$\sigma_A \ll \delta \leqslant \delta_0 \approx 0.2d \text{ and } \Delta E(\delta) < \Delta E_0(\delta_0) \tag{3.11}$$

is satisfied. From equations (3.9)–(3.11), one can expect, in agreement with observations [8], that T_s is lower than the temperature T_0 at which the anomalies in the Mössbauer spectral intensity were observed. In section 4 we find numerical values of $T_s \approx 500$ K and $\delta T \approx 50$ K (also in agreement with experimental data).

It should be noted that a further rise in the temperature T above T_s does not change markedly the ECD $|\Psi_f(0)|^2$ at the Mössbauer nuclei. Therefore, at higher temperatures $T^{(H)} > T_s$ the effective Mössbauer line shift (including the SLEF-generated ARCOMIS) exhibits the 'normal' temperature dependence parallel to that at low $T^{(L)} < T_s$ but with a higher magnitude caused by the ARCOMIS at T_s. This conclusion is in agreement with experimental observations [8].

The temperature interval δT around T_s within which the ARCOMIS occurs can be found from the equation

$$\delta T \approx T_s/A^{3/2} \text{ or } \delta T \approx 0.12T_s \tag{3.12}$$

(for $A \approx 4$) similar to that discussed in our previous work [9]. Equation (3.12), yielding $\delta T \approx 60$ K at $T_s \approx 500$ K (found in the next section), is in agreement with experimental observations for Ag–Sn alloys [8].

4. Comparison of calculated and experimental critical temperature for anomalies in the Mössbauer isomer shift

Here we calculate numerically the critical temperature T_s (equation (3.9)) around which the Mössbauer line shift increases abnormally within a relatively narrow temperature interval $\delta T \ll T_s$ (equation (3.12)). For this purpose we find ΔE from the relation

$$\Delta E(\delta)/\Delta E_0(\delta_0) \approx (\delta/\delta_0)^2 < 1 \tag{4.1}$$

resulting from equations (3.10) and (3.11). Then using equation (3.9) one obtains

$$T_s/T_0 \approx \Delta E(\delta)/\Delta E_0(\delta_0) \approx (\delta/\delta_0)^2 < 1. \tag{4.2}$$

Here ΔE_0, T_0 and δ_0 are the SLEF threshold energy, critical temperature and large atomic displacement related to the SLEF-induced anomalies in the Mössbauer spectral intensity [9]. We assume that the denominator in equation (3.9)

$$Z = k(\Delta S_{0p}/k + \delta S/k + 3\ln A) \approx Z_0 \tag{4.3}$$

is approximately equal to that, Z_0, calculated in [9] in the same alloy. The critical LTAD $\delta \gg \sigma_a$ (figure 2) can vary in a narrow interval limited by conditions (3.11), which can be rewritten in the 'numerical' form

$$\sigma_A(\text{Ag–Sn}) \approx 0.03d \ll \delta < \delta_0 \approx 0.2d \tag{4.4}$$

where $\delta_0 \approx 0.2d$ is the Lindemann atomic displacement [9].

Using equations (3.9) and (4.1)–(4.4) one can calculate T_s(Ag–Sn) in the following two interrelated ways. First, taking $\delta(\text{Ag}) \approx 0.15d < 0.2d$, one finds from equation (4.2)

$$T_s(\text{Ag–Sn}) \approx T_0(\text{Ag–Sn})\left[\frac{\delta(\text{Ag})}{\delta^0(\text{Ag})}\right]^2 = 506\ \text{K}. \tag{4.5}$$

Here T_0(Ag–Sn) $\approx$ 900 K [9]. The value T_s(Ag–Sn) in equation (4.5) is in good agreement with the experimental data for Ag–Sn alloys [8].

The second way of computation of T_s(Ag–Sn) leading to the same result is associated with the direct calculation of $\Delta E(\delta)$ from equation (3.10) and T_s from equation (3.9) for the same Ag–Sn alloy; here one can use the standard values for the bulk moduli B and average volume Ω_0 per atom, $Z \approx Z_0$ (equation (4.3)) and the same related value δ(Ag–Sn) $\approx 0.15d$. Then we find δT(Ag–Sn) from equation (3.12) using the numerical value for T_s(Ag–Sn) given by equation (4.5) and $A \approx 4$ [9]. This yields $\delta T(\text{Ag–Sn}) \approx T_s(\text{Ag–Sn})/A^{3/2} \approx 63$ K. The value for $\delta T \ll T_s$ is in good agreement with the experimental data found in the Ag–Sn system [8].

Using the two similar approaches and the results obtained in [9] for Au–Sn alloys, we calculate now T_s(Au–Sn) and δT(Au–Sn) for the Au–Sn alloys and compare the results of the calculations with tentative experimental data on the ARCOMIS observed in these materials. First, taking

$$\delta(\text{Au–Sn}) \approx 0.17d < \delta_0(\text{Au–Sn}) \approx 0.2d \tag{4.6}$$

according to condition (3.11), one finds from a relation similar to equation (4.2)

$$T_s(\text{Au–Sn}) \approx T_0(\text{Au–Sn})\left[\frac{\delta(\text{Au–Sn})}{\delta_0(\text{Au–Sn})}\right]^2 \approx 400\ \text{K}. \tag{4.7}$$

Here T_0(Au–Sn) $\approx$ 550 K [9] and δ_0(Au–Sn) $\approx 0.2d$ [9], and we assume that relations similar to equations (4.1)–(4.3) are also valid for the considered Au–Sn alloys. The calculated temperature T_s(Au–Sn) is in good agreement with tentative experimental observations for the Au–Sn alloys in question.

Then we find the narrow temperature interval (from equation (3.12)) δT(Au–Sn) $\approx$ $T_s(\text{Au–Sn})/A^{3/2} \approx 50$ K, which is also in good agreement with the observed $\delta T^{(obs)}$(Au–Sn) for these alloys (here $A \approx 4$ [9]).

5. The magnitude of the anomalous isomer shift

The complete detailed solution of the many-body time-dependent non-linear problem related to the ARCOMIS magnitude presents a formidable task. In this paper we limit ourselves to a qualitative and semiquantitative consideration which enables us to obtain a rough estimate of the SLEF-generated ARCOMIS magnitude.

According to our model, SLEFs of $\epsilon_{0p} \geqslant \Delta E \gg kT$ generate sequences of random dynamic arrays of simultaneously occurring non-equilibrium nanometre regions of volume $(Ad)^3$ which exist permanently in the solid. Each of these SLEF-distorted regions containing A^3 atoms (e.g. $A^3 = 64$ for $A = 4$ [9]) can localize Δn_t mobile electrons during the SLEF picosecond lifetime $\Delta\tau$ (as mentioned in the previous sections and [9, 12, 13, 15, 17–22, 25]). This enhances the local electron density $|\Psi_a|^2$ (per atom of the absorber) in the SLEF-excited nanometre region by $\Delta|\Psi_a|^2 \approx \Delta n_t/A^3$. Hence one can expect that in the presence of SLEFs the electron charge density $|\Psi_f(0)|^2$ at the Mössbauer nuclei is $|\Psi_f(0)|^2 \approx |\Psi_a(0)|^2 + \Delta n_t/A^3$. Then one finds (from equation (3.2)) the additional SLEF-generated shift in the Mössbauer line, i.e. the ARCOMIS magnitude

$$\Delta U_f \approx \alpha\Delta|\Psi_a|^2 \approx \alpha\Delta n_t/A^3. \tag{5.1}$$

According to this relation, the SLEF-induced ARCOMIS magnitude is determined by the average number Δn_t of mobile electrons localized in the SLEF-excited nanometre region $(Ad)^3$ and by parameter A (known as $A \approx 4$ [9]). The volume $(Ad)^3$ contains as many as $N_e \approx \gamma_v A^3$ valence electrons, where γ_v is the valence. Only a small part $kT/\epsilon_F \approx 10^{-2}$ of the valence electrons has energies above the Fermi level ϵ_F. Thus the number of such electrons per volume $(Ad)^3$ is $N_{eF} \approx \gamma_v A^3 kT/\epsilon_F \approx 10^{-2}\gamma_v A^3$ or $N_{eF} \approx 0.5$ for $A = 4$ [9], $\gamma_v(\mathrm{Ag, Au}) = 1$, $\epsilon_F(\mathrm{Ag, Au}) \approx 5.5$ eV and $T \approx 500$ K. Hence one can expect that a single electron ($\Delta n_t \approx 1$) can be localized in the immediate vicinity of the Mössbauer atom in every SLEF-excited nanometre region; the Coulomb repulsion prevents simultaneous localization of more than one electron in the immediate vicinity of the fluctuating atom. Thus taking $\Delta n_t \approx 1$ and $A^3 \approx 64$, one finds

$$\Delta U_f/\Delta U_{IS} \approx 10^{-2} \tag{5.2}$$

that is in good agreement with experimental data [8].

6. Concluding remarks and summary

Our nanoscopic dynamic fluctuations model suggests a stochastic dynamic mechanism for the recently observed anomalous reversible changes of the Mössbauer IS (ARCOMIS) [8]. The model is based on the nanoscopic kinetic theory of short-lived large energy fluctuations (SLEFs) (figure 1) and the SLEF-induced correlated picosecond atomic and electronic phenomena. They involve large non-linear transient atomic displacements (LTADs) $\Delta q_0 \gg \sigma_A$ (figure 2) and material distortion in nanometre material regions generating strong electron–lattice interactions [9, 12–25]. This causes transient electron localization in the nanometre vicinity of the Mössbauer impurity and induces the corresponding electron charge density (ECD) enhancement $|\Psi_f(0)|^2 - |\Psi_a(0)|^2$ at the Mössbauer nucleus (figure 3). The model shows the existence of the ARCOMIS at the critical temperature T_s, when the Mössbauer nuclei in the entire alloy are affected simultaneously and permanently by the 'anomalous' SLEF-generated increase in the ECD $|\Psi_f(0)|^2$ at the impurity concentration $b(\mathrm{Sn}) > 3\%$. Our model enables one to calculate the three main experimentally measurable parameters, namely, the transition temperature T_s, the narrow temperature interval $\delta T \ll T_s$ around T_s within which

the ARCOMIS takes place and the ARCOMIS magnitude. The calculated parameters are in good agreement with experimental data for the Ag–Sn and Au–Sn alloys.

The proposed model also enables one to understand why the ARCOMIS is not observed in SnO_2. This material is a dielectric with a wide forbidden gap and a very small concentration of free carriers at temperatures under consideration. Hence one concludes that the proposed ARCOMIS mechanism discussed in the previous sections and assuming the presence of mobile electrons is not applicable to SnO_2.

The suggested model is not designed *ad hoc* for the interpretation of the anomalies seen in the Mössbauer shift. This model is an extension of our previous SLEF-based models suggested earlier for the consideration of the anomalies found in the Mössbauer spectral intensity [9] and for the kinetics of many other processes in various systems [12–30, 36]. This suggests new possibilities for links between the SLEF-generated 'anomalies' in the Mössbauer spectroscopy and the kinetics of some other SLEF-induced phenomena in solids.

It seems worthwhile noting that the proposed model establishes new experimentally detectable links between the thermal SLEF-induced 'violent' non-linear correlated atomic and electronic motion in solids, on the one hand, and the behaviour of nuclear levels (whose energy is higher than the atomic SLEF energy by a few orders of magnitude), on the other.

In summary, a nanoscopic SLEF-based electron-related dynamic model for the observed anomalous temperature and Sn concentration dependences of the Mössbauer Sn isomer shift in the Ag–Sn [8] (and Au–Sn) alloys is suggested. Our model suggests explanations for the following experimental facts reported in [8].

(i) The existence of the anomalous reversible change of the Mössbauer isomer shift (ARCOMIS) in Ag–Sn (and Au–Sn) alloys around relatively low temperatures T_s, T_s(Ag–Sn) $\approx$ 500 K and T_s(Au–Sn) $\approx$ 400 K. The calculated critical temperature T_s around which the ARCOMIS takes place is in good agreement with observations.
(ii) The existence of the narrow temperature interval $\delta T \ll T_s$ (around T_s) within which the ARCOMIS takes place; calculated $\delta T \approx 0.1 T_s$ is in good agreement with experiments.
(iii) The magnitude of the ARCOMIS has been calculated, and agreement between calculations and observations has been found.
(iv) The model suggests an explanation of why the ARCOMIS appears in the Ag–Sn and Au–Sn alloys only when the Sn concentration becomes higher than 3%.
(v) An explanation for the absence of the ARCOMIS in SnO_2 oxides is suggested.
(vi) Our model shows that the ARCOMIS results from simultaneously and permanently occurring SLEF-induced electron localization in the nanometre vicinities of the Mössbauer atoms in the entire alloy enhancing the electron charge density (ECD) $|\Psi_f(0)|^2$ at the Mössbauer nuclei (figure 3).

Acronyms

SLEF—short-lived large energy fluctuation.
ARCOMIS—anomalous reversible change of the Mössbauer isomer shift.
ECD—electron charge density.
HFA—hyperthermal fluctuating atom.
LTAD—large transient atomic displacement.

References

[1] Johnson R A 1990 *Phys. Rev.* B **41** 9717

[2] Martin C H and Singer S J 1991 *Phys. Rev.* B **44** 477
[3] Cai J and Yee Y Y 1996 *Phys. Rev.* B **54** 8398
[4] Haskel D, Shechter H, Stern E A, Newville M and Yacoby Y 1993 *Phys. Rev.* B **47** 14 032
[5] Shechter H, Stern E A, Yacoby Y, Brener R and Zhang Z 1989 *Phys. Rev.* B **63** 1400
[6] Stern E A and Zhang Z 1988 *Phys. Rev.* B **60** 1872
[7] Stern E A, Linins P and Zhang Z 1991 *Phys. Rev.* B **43** 8850
[8] Shechter H, Haskel D, Stern E A and Yacoby Y 1998 *J. Phys.: Condens. Matter* **10** 9
[9] Khait Yu L, Snapiro I B and Shechter H 1995 *Phys. Rev.* B **52** 9392
[10] Frauenfelder H 1962 *The Mössbauer Effect* (New York: Benjamin)
Gibbs T C 1976 *Principles of Mössbauer Spectroscopy* (London: Chapman and Hall)
[11] Goldanski V I and Gerber R H 1968 *Chemical Applications of the Mošsbauer Spectroscopy* (New York: Academic)
Shenoy K and Wagner F E 1978 *Mössbauer Isomer Shift* (Amsterdam: North-Holland)
McGervey I D 1983 *Introduction to Modern Physics* (New York: Academic)
[12] Khait Yu L 1983 *Phys. Rep.* **99** 237
Khait Yu L 1988 *Recent Progress in Many-Body Theories* ed A Y Kallio *et al* (New York: Plenum)
[13] Khait Yu L, Brener R and Beserman R 1988 *Phys. Rev.* B **38** 6107
[14] Khait Yu L 1980 *Physica* A **103** 1
[15] Khait Yu L, Beserman R, Shaw D and Dettmer K 1994 *Phys. Rev.* B **50** 14 893
[16] Khait Yu L, Silberman A, Weil R and Adler J 1991 *Phys. Rev.* B **44** 8308
Khait Yu L, Silberman A, Weil R and Adler J 1998 *J. Non-Cryst. Solids* **137/138** 145
Rao K R 1998 *Curr. Sci.* **75** 1328
[17] Khait Yu L 1997 *Kinetics and Application of Atomic Diffusion in Solids: Nanoscopic Electron-Related Stochastic Dynamics* (Switzerland: Scitec)
[18] Khait Yu L and Beserman R 1986 *Phys. Rev.* B **33** 8107
Khait Yu L and Weil R 1995 *J. Appl. Phys.* **78** 6504
[19] Khait Yu L, Weil R, Beserman R, Beyer W and Wagner W 1990 *Phys. Rev.* B **42** 9000
[20] Khait Yu L 1991 *Semicond. Sci. Technol.* C **6** 84
[21] Khait Yu L and Richter V 1993 *J. Phys. D: Appl. Phys.* **26** 8306
[22] Khait Yu L, Saltzman J and Beserman R 1988 *Appl. Phys. Lett.* **53** 2235
[23] Khait Yu L 1988 *Z. Phys.* B **71** 8
[24] Khait Yu L 1986 *Physica* B **139** 237
[25] Khait Yu L and Snapiro I 1997 *Unsolved Problems of Noise* ed Ch R Doering, L B Kiss and M F Schlesinger (Singapore: World Scientific)
[26] Dettmer K, Freiman W, Levy M, Khait Yu L and Beserman R 1995 *Appl. Phys. Lett.* **66** 237
[27] Freiman W, Beserman R, Khait Yu L, Shanan M, Dettmer K and Kessler F R 1993 *Phys. Rev.* B **48** 14 893
[28] Khait Yu L, Salzman J and Beserman R 1989 *Appl. Phys. Lett.* **55** 1170
[29] Salzman J, Khait Yu L and Beserman R 1989 *Electron. Lett.* **25** 244
[30] Freiman W, Eyal A, Khait Yu L and Beserman R 1996 *Appl. Phys. Lett.* **69** 3821
[31] Kittel C 1975 *Quantum Theory of Solids* (New York: Wiley)
[32] Ziman J N (ed) 1969 *The Physics of Metals* (Cambridge: Cambridge University Press)
[33] Ashcroft N W and Mermin N D 1975 *Solid State Physics* (New York: Holt, Rinehart and Winston)
[34] Kittel C 1976 *Introduction to Solid State Physics* (New York: Wiley)
[35] Frenkel 1946 *Kinetic Theory of Liquids* (Oxford: Clarendon)
[36] Yukalov V I 1991 *Phys. Rep.* **208** 393